Proceedings of the Seventh International Conference on
Railway Technology: Research, Development and Maintenance
Edited by: J. Pombo
Civil-Comp Conferences, Volume 15, Paper 22.1
Civil-Comp Press, Edinburgh, United Kingdom, 2026
ISSN: 2753-3239, doi: 10.4203/ccc.15.22.1

Enhancement of Rail Wear Resistance and Fatigue Toughness through Discrete Surface Quenching and Low-Temperature Ageing

T. Bai[1,2], K. Wang[3], J. Xu[1,2] and P. Wang[1,2]

[1]MOE Key Laboratory of High-speed Railway Engineering, Southwest Jiaotong University, Chengdu, China
[2]School of Civil Engineering, Southwest Jiaotong University, Chengdu, China
[3]College of Design and Engineering, National University of Singapore, Singapore

Abstract

This paper proposes a rail surface heat treatment method to mitigate wear and fatigue damage. Discrete quenching is first applied to the rail surface using a high-energy plasma beam, producing a high-hardness hardened layer. Subsequently, ageing treatment is carried out at 270 °C to achieve a smooth hardness transition between the hardened layer and the rail substrate. Microscopic observations show that, after quenching, the microstructure within the hardened layer consists of high-strength and high-hardness acicular martensite, with a hardness reaching 2.3 times that of the pearlitic substrate. After low-temperature ageing, carbide precipitation occurs within the martensite, and the microstructure transforms into tempered martensite. Combined electron backscatter diffraction analysis indicates that, after ageing treatment, lattice distortion and dislocation density at the boundary of the hardened layer decrease, thereby improving the deformation compatibility between the hardened layer and the substrate. Twin-disc wheel-rail test results show that rail wear is reduced by more than 50% after quenching. Meanwhile, the ageing treatment effectively prevents severe fatigue cracking in quenched rails. After the heat treatment, both wear and fatigue crack damage of the rail are alleviated, significantly extending the service life of the rail.

Keywords: rail, discrete quenching, low-temperature ageing, gradient hardening, wear resistance, fatigue toughness.

1 Introduction

Rails are key infrastructure components in railway systems. On the one hand, rails are in direct contact with wheels and bear the loads transmitted by trains. On the other hand, rails provide guidance for train operation and ensure the running direction. Under train loading, rail surfaces are prone to wear and rolling contact fatigue cracks. These forms of damage intensify the wheel–rail interaction [1], affecting train running stability and the service life of rails. In severe cases, they may lead to safety accidents such as derailment [2]. Therefore, mitigating rail wear and fatigue damage is of great significance for extending rail service life and ensuring safe railway operation.

A variety of methods are proposed to extend the service life of rails, including wheel–rail profile grinding [3], laser cladding [4], and surface quenching [5]. These approaches effectively mitigate rail damage. Among them, rail surface quenching is a heat treatment method characterised by low energy consumption, high efficiency, and controllable cost [5], and it has attracted extensive research attention in recent years.

Rail surface quenching utilises the austenitic phase transformation and the martensitic phase transformation of the pearlitic substrate to generate discretely distributed hardened layers [6]. By utilising the high strength and high hardness of the martensitic microstructure, rail wear is reduced. Existing studies show that the wear resistance of rails after quenching treatment increases by more than twofold [7]. Although the improvement in rail wear resistance after quenching is widely confirmed [8], owing to the large hardness difference between the martensitic microstructure in the hardened layer and the pearlitic microstructure of the substrate, pronounced fatigue cracks are prone to occur at the edges of the hardened layer [9]. This hardness difference is considered to be the key factor leading to crack initiation [10].

In recent years, a small number of researchers focus on the hardness difference between the hardened layer and the substrate and propose methods such as induction-assisted laser quenching [11] and laminar plasma tempering [12] to mitigate fatigue damage at the edges of the hardened layer. These methods mainly apply secondary heating to the hardened layer at temperatures above 400 °C, thereby reducing the hardness difference between the hardened layer and the substrate. However, the reasons and mechanisms responsible for hardness reduction and damage mitigation after repeated heat treatment still require further investigation, and the reduction in hardness also has an adverse effect on the improvement of wear resistance. At the same time, a secondary heating temperature of 400 °C is relatively high, which is unfavourable for the control of energy consumption and cost.

In our study, a combined heat treatment method employing discrete surface quenching and low-temperature ageing is proposed. Ageing treatment is applied to the hardened layer after discrete quenching at a temperature of 270 °C, thereby reducing the hardness difference between the hardened layer and the substrate. The microstructures of the hardened layer after quenching and after low-temperature ageing are respectively characterised, and the crystallographic characteristics at the edge of the hardened layer are analysed, revealing the mechanism by which low-temperature ageing leads to hardness reduction. Combined with twin-disc wheel–rail tests, the effects of discrete quenching and low-temperature ageing on rail wear and fatigue damage are investigated. This research provides theoretical support for the application of heat treatment technologies in extending rail service life.

2 Methods

The materials used in the experiments are taken from CL60 railway wheels and U75V rails and are machined into discs with a diameter of 60 mm for twin-disc wheel–rail testing. First, rail specimens are subjected to quenching treatment using a laminar plasma beam, with the plasma power set to 6 kW and the processing time uniformly controlled at 0.35 s. Discretely distributed hardened layers are formed on the specimen surface, with a hardened layer diameter of 5.5 mm and a depth of 0.9 mm, arranged regularly at a spacing of 3 mm. Subsequently, the rail specimens are placed in a furnace at 270 °C for ageing treatment, with a holding time of 120 min. In this study, a total of three groups of wheel–rail specimens are prepared for comparison, while the material source and treatment of the wheel specimens remain unchanged. The rail specimens are designated as No. 1 (without heat treatment), No. 2 (discrete surface quenching), and No. 3 (low-temperature ageing after discrete surface quenching).

To evaluate the degree of wear and fatigue damage of rails after discrete quenching and low-temperature ageing, the three groups of wheel–rail specimens are subjected to rolling contact friction and wear tests on a twin-disc testing machine. The test parameters are determined according to the geometric and stress conditions of the Hertzian simulation criterion. The applied load is 5280 N, the slip ratio is 5%, and the total number of cycles is set to 200,000 revolutions. Figure 1 presents the specimen processing procedure and the details of the twin-disc tests.

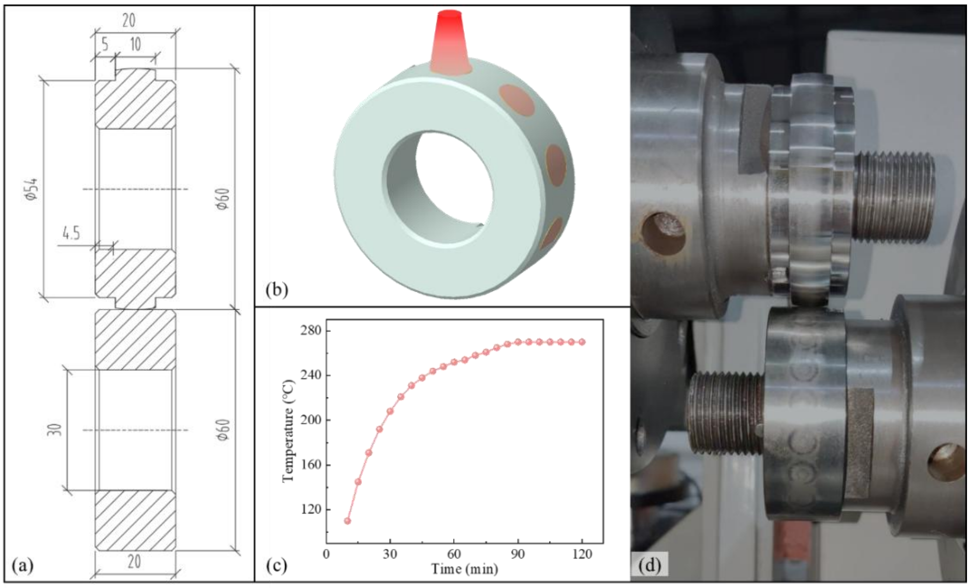

Figure 1: Experimental procedure: (a) specimen dimensions; (b) discrete surface quenching of the rail specimen; (c) temperature variation curve during low-temperature ageing treatment; (d) twin-disc wheel–rail test.

Before the tests, the microstructure of the hardened layer is observed using an optical microscope (OLS5100, OLYMPUS, Japan) and a scanning electron microscope (JSM-IT500, JEOL, Japan). At the same time, electron backscatter diffraction is employed to characterise the grain orientation at the boundary of the hardened layer. After the tests, the weight loss of the rail specimens is calculated as an indicator for evaluating wear. The specimen surface and the section along the rolling direction are cut to obtain small samples with dimensions of 5 × 5 × 3 mm. After grinding, polishing, and etching, the fatigue damage on the specimen surface and sections is examined using optical microscopy and scanning electron microscopy.

3 Microstructure of Rails after Heat Treatment

Changes in microstructure are the fundamental reason for variations in mechanical properties and damage characteristics of materials. Optical microscopy (OM) and scanning electron microscopy (SEM) are first used to characterise the microstructures of the three rail specimens subjected to different treatments, as shown in Figure 2. Figure 2(a) shows the microstructure of the specimen without heat treatment, which appears as lamellar pearlite composed of alternating ferrite and cementite under high-magnification SEM, representing the typical microstructural characteristic of U75V rail steel.

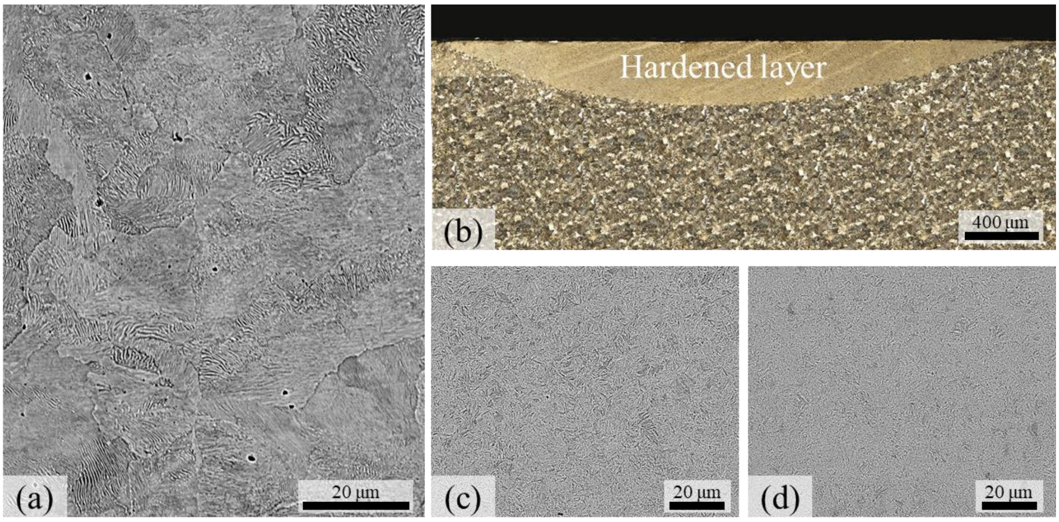

Figure 2: Microstructures of rail specimens: (a) SEM image of specimen No. 1; (b) OM image of specimen No. 2; (c) SEM image of specimen No. 2; (d) SEM image of specimen No. 3.

Figure 2(b) shows the morphological features of the hardened layer observed under low-magnification OM. After quenching, a crescent-shaped hardened layer forms on the rail surface, and a clear boundary exists between the hardened layer and the substrate due to their different corrosion resistance. Figure 2(c) presents the microstructure of the hardened layer observed under high-magnification SEM. During quenching, the original pearlitic substrate undergoes rapid heating and cooling, leading to austenitic transformation followed by martensitic transformation. The microstructure within the hardened layer consists of acicular martensite with randomly distributed orientations, together with a small amount of retained austenite. Owing to the rapid cooling process, supersaturated carbides remain within the martensite without sufficient precipitation, resulting in significantly higher strength and hardness of the martensitic microstructure compared with the pearlitic substrate. Figure 2(d) shows the high-magnification SEM image of the hardened layer after low-temperature ageing treatment. After low-temperature ageing, the acicular martensite in the hardened layer decomposes and transforms into finer tempered martensite, while part of the supersaturated carbides precipitates. This microstructural evolution leads to a reduction in hardness and an improvement in toughness.

To better understand the influence of ageing treatment on the mechanical properties of the hardened layer, EBSD analyses are conducted on the hardened layer and at the boundary of the hardened layer, as shown in Figure 3. Figures 3(a) and (b) present the dislocation density distribution within the hardened layer. After quenching, the dislocation density inside the hardened layer is relatively high, indicating that the material exhibits high strength and hardness with limited deformability. After low-temperature ageing treatment, the dislocation density within the hardened layer decreases, leading to a reduction in material strength and hardness, while the plastic deformation capability is enhanced. Figures 3(c) and (d) show the KAM maps at the boundary of the hardened layer, which reflect the degree of lattice distortion. After quenching, severe lattice distortion is observed at the hardened layer boundary, indicating that cracks are prone to initiate in this region. After low-temperature ageing treatment, the degree of lattice distortion at the hardened layer boundary decreases, indicating that ageing treatment improves the material toughness.

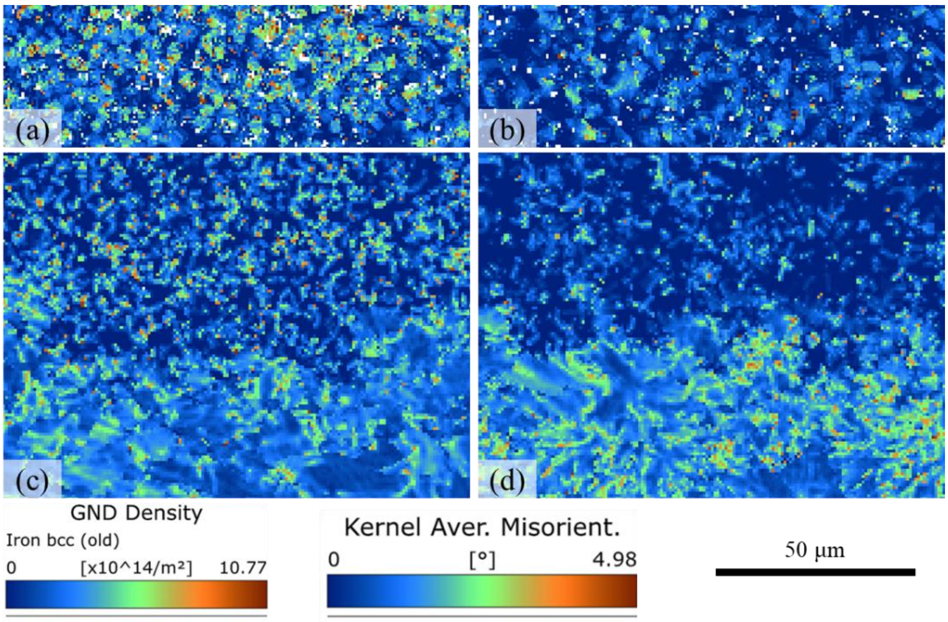

Figure 3: EBSD results of rail specimens: (a) GND density map of specimen No. 2; (b) GND density map of specimen No. 3; (c) KAM map of specimen No. 2; (d) KAM map of specimen No. 3.

To visually illustrate the effect of low-temperature ageing on material hardness, the hardness distribution along the depth direction at the centre of the hardened layer on the rail longitudinal section is measured, as shown in Figure 4. After quenching, the hardness of the hardened layer increases significantly, reaching 880 $HV_{0.5}$, which is 2.3 times that of the pearlitic substrate (380 $HV_{0.5}$). This is mainly attributed to the solid solution within the martensite and the high dislocation density. Meanwhile, at the boundary of the hardened layer, the hardness decreases rapidly. Under conditions of a large hardness difference and severe lattice distortion, fatigue cracks are prone to initiate at the boundary. After low-temperature ageing treatment (Figure 4(b)), the hardness of the pearlitic substrate remains unchanged, while the hardness of the hardened layer decreases. This is mainly due to the refinement of the martensitic microstructure and the reduction in dislocation density. As a result, the hardness difference at the boundary of the hardened layer is reduced, which helps to alleviate fatigue damage at the hardened layer boundary.

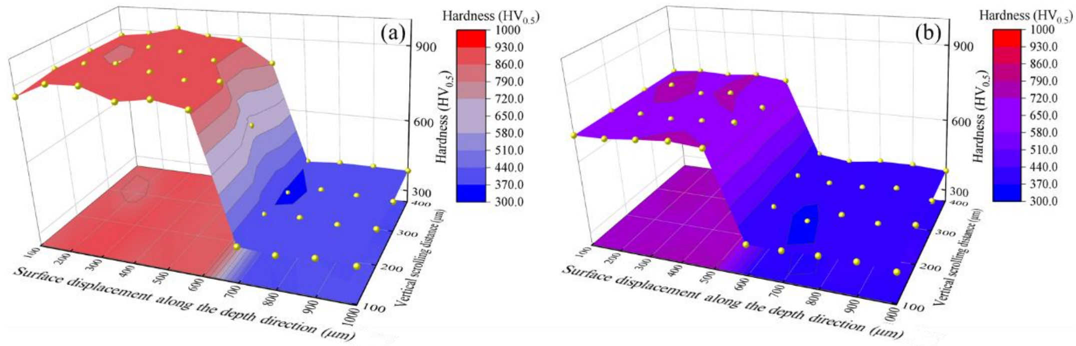

Figure 4: Hardness distribution of the hardened layer along the depth direction: (a) specimen No. 2; (b) specimen No. 3.

4 Results

To determine the effects of low-temperature ageing treatment on rail wear and fatigue damage, the weight loss of the rail specimens before and after the tests is measured, and OM and SEM are used to observe the surface and sectional morphologies and crack characteristics of the rail specimens. Figure 5 presents the weight loss of the rail specimens. After quenching, the rail specimen (No. 2) shows a weight loss reduction of 59.7%, indicating that quenching heat treatment significantly improves rail wear resistance. This is mainly attributed to the acicular martensitic microstructure in the hardened layer, which exhibits much higher hardness than the pearlitic substrate. After low-temperature ageing treatment (No. 3), the weight loss of the rail increases due to the reduction in material hardness. However, compared with the untreated rail specimen (No. 1), the weight loss still decreases by 40.7%. This indicates that, after quenching combined with low-temperature ageing treatment, the wear resistance of the rail is still significantly improved.

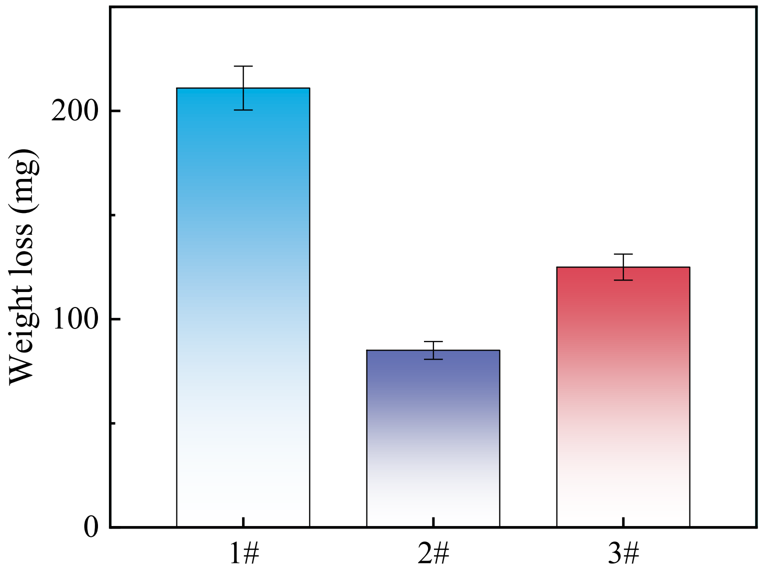

Figure 5: Weight loss of rail specimens.

Figure 6 presents SEM images of the surface morphologies of the rail specimens. For the untreated rail specimen (No. 1), the surface exhibits lamellar spalling, which is mainly generated under the repeated action of wheel–rail contact stress and shear stress. After quenching treatment (No. 2), large spalling pits appear at the boundary of the hardened layer, accompanied by a large number of lateral cracks. This is mainly due to the large hardness difference between the hardened layer and the substrate, which leads to deformation incompatibility on both sides and consequently results in severe fatigue damage. After low-temperature ageing treatment (No. 3), the reduction in hardness leads to a smoother transition on both sides of the hardened layer, and no obvious material detachment or severe lateral cracks are observed at the boundary. The surface morphologies of both the hardened layer and the substrate exhibit lamellar spalling, indicating that low-temperature ageing treatment improves the rolling contact fatigue toughness of the material.

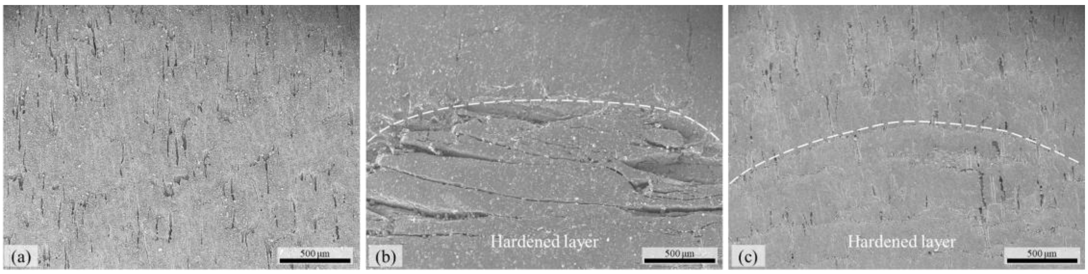

Figure 6: Surface morphologies of rail specimens: (a) specimen No. 1; (b) specimen No. 2; (c) specimen No. 3.

Furthermore, Figure 7 shows the rolling contact fatigue damage characteristics on the longitudinal sections of the rail specimens along the rolling direction. For the untreated rail specimen (No. 1), under the repeated action of contact stress and shear stress, plastic deformation occurs in the surface pearlitic microstructure, with an affected depth of 58.6 μm and a direction along the rolling direction. Meanwhile, rolling contact fatigue cracks appear at the rail surface, and the cracks propagate into the interior at an angle of 8.4°, with a depth of 10.7 μm. For the quenched rail specimen (No. 2), severe spalling and vertical cracks appear at the boundary of the hardened layer, while no obvious plastic deformation is observed on the surface of the hardened layer. Due to the large hardness difference between the hardened layer and the substrate, the deformation coordination ability at the boundary is weak, resulting in significant impact and stress concentration at the boundary and leading to crack initiation. At the same time, the hardened layer exhibits high dislocation density and severe lattice distortion, with poor deformability, causing cracks to propagate into the rail interior at angles of 70°–90°. The crack depth reaches 393.3 μm. When cracks propagate to the boundary, owing to the good toughness of the pearlitic substrate, crack deflection occurs at the boundary, and the cracks propagate along the boundary. Subsequently, when cracks intersect and coalesce, large-area spalling occurs. After low-temperature ageing treatment (No. 3), the hardness difference and lattice distortion at the boundary are reduced, and the deformation coordination ability is improved. No obvious vertical cracks or spalling are observed at the hardened layer boundary. In addition, due to the reduction in dislocation density and the enhancement of deformability in the hardened layer, a plastic deformation zone with a depth of 25 μm is observed near the surface of the hardened layer, together with inclined cracks propagating inward at angles of 10°–13°, with a depth of 9.1 μm. The rolling contact fatigue crack characteristics are essentially consistent with those of the untreated specimen (No. 1), indicating that the fatigue toughness of the material is improved after low-temperature ageing treatment.

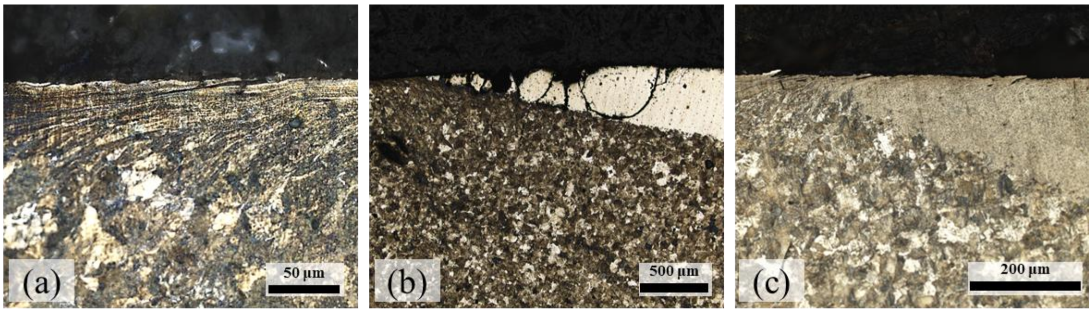

Figure 7: Crack characteristics on the longitudinal sections of rail specimens: (a) specimen No. 1; (b) specimen No. 2; (c) specimen No. 3.

5 Conclusions and Contributions

In this study, in order to improve the wear resistance of rails while maintaining a certain level of fatigue toughness, a synergistic heat treatment method combining discrete surface quenching and low-temperature ageing is proposed. Discretely distributed hardened layers are introduced by surface quenching to mitigate rail wear. Low-temperature ageing treatment is further applied to reduce the hardness difference between the hardened layer and the substrate, thereby alleviating fatigue damage. According to the results of this study, after quenching, the hardened layer exhibits an acicular martensitic microstructure with high hardness and high dislocation density, and a hardness difference of 500 HV0.5 exists at the boundary of the hardened layer, accompanied by severe lattice distortion. After low-temperature ageing treatment, solute precipitation occurs within the martensite, and the hardness and dislocation density decrease, while the hardness difference and lattice distortion at the boundary are alleviated. The twin-disc test results show that the application of this combined heat treatment method reduces rail weight loss by 40.7%. Meanwhile, the extensive cracking and spalling observed at the hardened layer boundary are mitigated, and the damage of the hardened layer manifests as rolling contact fatigue inclined cracks similar to those in the substrate.

Acknowledgements

The authors would like to thank the National Natural Science Foundation of China (U2568212, 52478474) for the financial support.

References

[1] X.S. Jin, Z.F. Wen, K.Y. Wang, Z.R. Zhou, Q.Y. Liu, C.H. Li, "Three-dimensional train–track model for study of rail corrugation", Journal of Sound and Vibration, 293(3), 830-855, 2006.

[2] T. Vernaillen, L. Wang, A. Núñez, R. Dollevoet, Z.L. Li, "Rail wear rate on the Belgian railway network – a big-data analysis", International Journal of Rail Transportation, 12(5), 765-780, 2024.

[3] M. Mesaritis, P. Cuervo, J.F. Santa, A. Toro, R. Lewis, "Assessment of rail grinding maintenance surface quality and damage propagation in subsequent loading cycles for premium rail grades", Wear, 530-531, 205051, 2023.

[4] A.S. Nellian, J.H.L. Pang, "Laser metal deposition characterization study of metal additive manufacturing repair of rail steel specimens", Virtual and Physical Prototyping, 18(1), e2134042, 2023.

[5] J.M. Xu, K. Wang, X.Y. Liang, Q. Guo, P. Wang, R. Chen, D.F. Zeng, G.D. Cui, F.H. Li, J. Guo, L. Li, "Investigation on wear and damage characteristics of high-speed rail steel with plasma selective quenching", Wear, 486-487, 204100, 2021.

[6] C.R. Su, L.B. Shi, W.J. Wang, D.Z. Wang, Z.B. Cai, Q.Y. Liu, Z.R. Zhou, "Investigation on the rolling wear and damage properties of laser dispersed quenched rail materials treated with different ratios", Tribology International, 135, 488-499, 2019.

[7] J.Z. Zhao, H.C. Miao, Q.H. Kan, P.L. Fu, L. Ding, G.Z. Kang, P. Wang, "Numerical investigation on the rolling contact wear and fatigue of laser dispersed quenched U71Mn rail", International Journal of Fatigue, 143, 106010, 2021.

[8] X. Cao, L.B. Shi, Z.B. Cai, Q.Y. Liu, Z.R. Zhou, W.J. Wang, "Investigation on the microstructure and damage characteristics of wheel and rail materials subject to laser dispersed quenching", Applied Surface Science, 450, 468-483, 2018.

[9] B. Zhang, D.P. Yu, W.J. Song, K.M. Peng, G.Y. Wu, "The rolling-sliding wear behavior and damage mechanism of the rail steel treated by plasma selective quenching", Surface and Coatings Technology, 428, 127908, 2021.
[10] Y. Gao, S.G. Wang, J.M. Xu, Y.B. Liu, Z.G. Dong, P. Wang, F. Yang, "Numerical investigation of crack initiation on rail surfaces considering laminar plasma quenching technology", Tribology International, 154, 106755, 2021.
[11] L. Meng, C. Xian, B.B. Zhu, R. Yan, Q.W. Hu, X.Y. Zeng, D.Z. Wang, "Comparison on the microstructure, bending properties and tribological behaviors of rail materials treated by laser dispersed quenching and induction assisted laser dispersed quenching", Surface and Coatings Technology, 410, 126936, 2021.
[12] K.M. Peng, D.P. Yu, P. Zhang, L.C. Wang, Z.H. Liao, Z.Q. Lu, G.Y. Wu, C.F. Song, L. Li, "Laminar plasma quenching-tempering: A rapid surface heat treatment technique for controllable modification of the rail steel", Surface and Coatings Technology, 473, 130029, 2023.